Ecosystems (2014) 17: 1186–1201
DOI: 10.1007/s10021-014-9786-0

ECOSYSTEMS

Partitioning Climatic and Biotic Effects on Interannual Variability of Ecosystem Carbon Exchange in Three Ecosystems

Junjiong Shao,[1,2] Xuhui Zhou,[1]* Honglin He,[2] Guirui Yu,[2]* Huimin Wang,[2] Yiqi Luo,[1,3] Jiakuan Chen,[1] Lianhong Gu,[4] and Bo Li[1]

[1]*Coastal Ecosystems Research Station of Yangtze River Estuary, Ministry of Education Key Laboratory for Biodiversity Science and Ecological Engineering, Institute of Biodiversity Science, Fudan University, 220 Handan Road, Shanghai 200433, China;* [2]*Institute of Geographical Sciences and Natural Resource Research, Chinese Academy of Sciences, 3 Datun Road, Beijing 100101, China;* [3]*Department of Microbiology and Plant Biology, University of Oklahoma, Norman, Oklahoma 73019, USA;* [4]*Oak Ridge National Laboratory, Oak Ridge, Tennessee 37831, USA*

Abstract

Understanding the climatic and biotic controls of interannual variability (IAV) in net ecosystem exchange (*NEE*) is important for projecting future uptake of CO_2 in terrestrial ecosystems. In this study, a statistical modeling approach was used to partition climatic and biotic effects on the IAV in *NEE*, gross primary productivity (*GPP*) and ecosystem respiration (*RE*) at a subtropical evergreen plantation in China (QYZ), a deciduous forest (MOZ), and a grassland (DK1) in the USA. The climatic effects in the study are defined as the interannual anomalies in carbon (C) fluxes directly caused by climatic variations, whereas the biotic effects are those caused by the IAV in photosynthetic and respiratory traits. The results showed that the contribution of biotic effects to the IAV in *NEE* increased significantly as the temporal scale got longer from daily to annual scales. At the annual scale, the contribution of biotic effects to the IAV in *NEE* was 47, 69, and 77% at QYZ, MOZ, and DK1, respectively. However, the IAV in *NEE* was mainly controlled by *GPP* at QYZ, and by *RE* at DK1, whereas the contributions of *GPP* and *RE* to the IAV in *NEE* were similar at MOZ, indicating different mechanisms regulating the IAV in *NEE* among ecosystems. Interestingly, there was a strong negative correlation between the climatic and biotic effects at the annual scale from 2003 to 2009 at QYZ ($r^2 = 0.80$, $P < 0.01$), suggesting these two effects counteracted each other and resulted in a relatively stable C sink, whereas no correlations were found at the other two sites. Overall, our study revealed the relative importance of climatic and biotic effects on the IAV in *NEE* and contributed to our understanding of their underlying mechanisms.

Key words: biotic effects; climatic effects; eddy covariance; interannual variability; net ecosystem exchange; relative contribution.

Received 11 December 2013; accepted 11 May 2014;
published online 24 June 2014

Electronic supplementary material: The online version of this article (doi:10.1007/s10021-014-9786-0) contains supplementary material, which is available to authorized users.

Author contributions JS, XZ, HH, GY, YL and BL conceived of and designed this study. JS, GY, HW, and LG performed the research. JS analyzed the data. JS and HH contributed new methods or models. JS, XZ, YL, JC, and BL wrote the paper.

*Corresponding author; e-mail: zxuhui14@fudan.edu.cn; yugr@igsnrr.ac.cn

Introduction

The Earth's climate is warming as a result of rapidly increasing CO_2 emissions and the global mean temperature is expected to increase by 1.1–6.4°C by the end of this century (IPCC 2007). Although nearly 30% of carbon (C) released by anthropogenic activities is sequestered by terrestrial ecosystems (Canadell and others 2007), whether this natural sink will be sustainable into the future is a major concern (Luo and Weng 2011). The capacity of ecosystem C sequestration depends on the magnitude of net ecosystem exchange of CO_2 (*NEE*), which usually varies among years. Large interannual variability (IAV) in *NEE* has been observed at almost all eddy-flux sites over the world (Baldocchi 2008).

Climatic variables, such as solar radiation, temperature, and water conditions (Barr and others 2007; Pintér and others 2008; Yuan and others 2009) as well as cloud cover, drought, snow cover, and El Niño-Southern Oscillation (ENSO, Baldocchi and others 2001; Goulden and others 1996; Weber and others 2009), are believed to be the direct drivers of the variation in *NEE*. However, climatic variables can also indirectly drive IAV in *NEE* by regulating ecological and physiological processes such as photosynthetic and respiratory traits (Humphreys and Lafleur 2011) and phenological features (for example, growing season length, transition dates, and phenological lags, Dragoni and others 2011; Richardson and others 2009; Wu and others 2013). In addition, stand age and nutrient conditions may also change ecophysiological properties (Buchmann and Schulze 1999; de Beeck and others 2010). In this paper, we defined the effects of ecological and physiological changes on IAV in C fluxes caused by either climate or other factors such as biotic effects. The direct effects of climatic variations were treated as climatic effects. Due to the complex interactions between the climate and ecophysiological processes, few studies have explicitly quantified the two types of effects on IAV in *NEE*, separately.

Over the past decade, two statistical approaches, the homogeneity-of-slopes method (Hui and others 2003) and the crossed model (Richardson and others 2007) have been developed to address the issue. Both methods apply models that simulate C fluxes with yearly varying parameters, and both consider the variation of *NEE* from changes of model parameters as biotic effects and those directly from changes of climatic variables as climatic effects. Analysis of variance (ANOVA) is then used to obtain the relative importance of the biotic and climatic effects in both methods. However, the multiple linear regression model used in Hui and others (2003) produced considerable model-data mismatch in some ecosystems (Polley and others 2008; Teklemariam and others 2010). Richardson and others (2007) used a process-based model to estimate the relative importance of climatic and biotic effects as well as the magnitude of the two effects each year, which has been successful for Howland forest, USA, but may not be suitable for other ecosystems. Thus, more flexible methods need to be developed with site-specific data sets.

Previous studies with these approaches have found that biotic effects became more important as the temporal scale increased from days to years (Hui and others 2003; Polley and others 2008; Richardson and others 2007), whereas climatic effects, mainly at diel to seasonal scales, had the opposite trend (Baldocchi 2008; Luo and Weng 2011). Moreover, the importance of biotic effects to IAV in *NEE* varied among ecosystems (for example, grassland > forest > peatland, Hui and others 2003; Polley and others 2008; Teklemariam and others 2010), and between deciduous and evergreen forests (deciduous > evergreen, Richardson and others 2007; Wu and others 2012).

Forest plantations, occupying about 200 million ha over the world (FAO 2007), are a large wood production and efficient C sink due to fast growth (Carle and Holmgren 2008; Pan and others 2011). In terms of area, China has the largest portion of global plantations (about one-third), 40% of which are planted in Southern and Eastern China with a subtropical monsoon climate (Huang and others 2012). However, the potential C sequestration in plantations was questioned by a recent meta-analysis, suggesting that soil C concentration in plantation forests was lower than that in natural forests (for all trees and the Genus *Pinus*, Liao and others 2012). Understanding this inconsistency requires more detailed studies on mechanisms of C cycling in plantations and their biotic responses to climate change, to which the partitioning of climatic and biotic effects would provide useful information.

Therefore, in this study, we aimed to investigate the relative importance of biotic and climatic effects on IAV in *NEE* and their potential interactions at a subtropical evergreen plantation in China. Instead of using the specific-scale functions in Richardson and others (2007), we applied the Bayesian information criterion (BIC) to optimize the relationships of climatic variables with maximum photosynthetic rate (A_m) and temperature sensitivity (Q_{10}) using multiple regression models. An empirical model with the optimized relationships and yearly varying

parameters was then constructed to simulate seasonality and IAV in *NEE*. A modified statistical approach from Richardson and others (2007) was used to partition the climatic and biotic effects on IAV in *NEE* (and its component fluxes *GPP* and *RE*) and their relative importance. Because the response magnitude of C fluxes to climate variability is the sum of biotic and climatic effects, the correlation between biotic and climatic effects can potentially reveal the possible responses of the ecosystem C cycle to future climate change and help clarify whether a positive feedback exists between the C cycle and climatic change (Cox and others 2000; Luo and others 2009). If the biotic effects are negatively correlated with climatic effects with similar magnitudes, ecosystem C fluxes may not fluctuate with climatic change and can be a robust C sink/source. To evaluate the performance of our modeling method, we also applied our approach to another two ecosystems, an oak forest and a C_3 grassland in the US. The three sites not only represent different ecosystem types (evergreen and deciduous forests, and grasslands), but also cover a wide range of geography and climate. Therefore, the comparison of the results across the three ecosystems will strengthen the application of our approach.

Methods

Site Information

In this study, we mainly focused on a subtropical plantation in China using a statistical modeling approach to examine climatic and biotic effects on IAV in C fluxes. Another two ecosystems in the USA were used to validate the approach. Thus, the three sites included Qianyanzhou, Missouri Ozark, and Duke Forest Open Field. The Qianyanzhou flux site (QYZ, 26°44′29″N, 115°03′29″E, a.s.l. 100 m) is located in Jiangxi Province, China. The site is controlled by a subtropical monsoon climate, whereas other areas at a similar latitude are occupied by arid steppes and deserts (Huang and others 2007). The mean annual temperature and precipitation are 17.9°C and 1,475 mm, respectively, based on the meteorological record from 1985 to 2007 (Wen and others 2010). High temperature and drought often occur in summer, suppressing plant physiological activities. The vegetation is a needle-leaved forest plantation that is 25 years old and approximately 13 m tall. The dominant species are *Pinus massoniana*, *Pinus elliottii*, and *Cunninghamia lanceolate*.

The Missouri Ozark flux site (MOZ, 38°44′39″N, 92°12′00″W, a.s.l. 219 m) is located at the Baskett Research and Education Area (BREA) in Missouri, USA. The climate of the area is warm, humid, and continental. The mean annual temperature and precipitation are 13.6°C and 1,023 mm over the period of 1971–2000, respectively. The vegetation is a deciduous forest that is 77 years old and approximately 13 m tall. The dominant species are white oak (*Quercus alba*) with other oak species and hickories (Yang and others 2010).

The Duke Forest Open Field (DK1, 35°58′16″N, 79°05′36″W, a.s.l. 168 m) is located at the Blackwood Division of the Duke forest in North Carolina, USA. The regional climate is characterized by warm and humid summers and mild winters with mean annual temperature of 15.5°C and mean annual precipitation of 1,145 mm based on the long-term record (111 years). The dominant species is the C_3 grass, *Festuca arundinacea* (Stoy and others 2008).

Data Sources

Half hourly data for *NEE* and corresponding climatic variables at the QYZ flux tower (2003–2009) were obtained from CERN (Chinese Ecosystem Research Network, www.cern.ac.cn/), whereas the data at MOZ (2005–2009) and DK1 (2003–2007) were from AmeriFlux (public.ornl.gov/ameriflux/index.html). These variables included F_c (CO_2 flux), u^* (friction velocity), *PAR* (photosynthetically active radiation), T_a (air temperature), T_s (soil temperature), *PPT* (precipitation), *SWC* (soil water content), and *VPD* (vapor pressure deficit).

Gap-Filling

The raw data were preprocessed by spike screening and nighttime filtering based on the methods in Papale and others (2006). Then a Q_{10} function was used to model the nighttime flux, which represents the nighttime ecosystem respiration (*RE*, Richardson and Hollinger 2005) and fill the gaps:

$$RE = R_{10} Q_{10}^{\frac{T_s - 10}{10}}, \quad (1)$$

where R_{10} is the respiration rate at 10°C, Q_{10} is the temperature sensitivity of *RE*. The parameterization of equation (1) follows the method from Reichstein and others (2005) with slight modifications. First, we set 1-month moving windows with a step of 1 day. If the valid nighttime data in a certain moving window were less than 100 points, the window was expanded to get enough data points. Then the fitted parameters R_{10} and Q_{10} were obtained for each moving window. Only the R_{10} values within a range of 0–0.15 mg C m^{-2} s^{-1} and the coefficient of variance (CV) less than 50% were

accepted (Reichstein and others 2005). These valid R_{10} values were averaged with the inverse of standard error as a weighting factor. The weighted R_{10} was considered as the long-term reference respiration rate through the whole period. Then we put the weighted R_{10}, a constant, into equation (1), and obtained the estimates of daily Q_{10} using 1-month moving window with a step of 1 day. Once the parameters in equation (1) were estimated, we applied it to fill the gaps at nighttime. Daytime *RE* was also estimated by this method to extend the equation to daytime.

GPP was estimated as the difference between estimated daytime *RE* and observed *NEE*. A Michaelis–Menten equation (Falge and others 2001) was used to describe the *GPP* for the daytime:

$$GPP = \frac{PAR \cdot A_m}{PAR + K_m}, \quad (2)$$

where A_m is the maximum photosynthetic rate and K_m is the Michaelis constant, which is *PAR* at which the photosynthetic rate is half of A_m. We fitted A_m and K_m using a 1-month moving window as described above to get the daily parameters of a photosynthesis model. We then used these parameters to estimate daytime *GPP*. The daytime flux gaps for *NEE* were filled by using the equation: $NEE = RE - GPP$.

Empirical Model

The seasonality of the parameters in the gap-filling model (for example A_m, R_{10} and Q_{10}) has been proven to be related to climatic variables (for example, temperature, soil moisture, and *VPD*) (Ricciuto and others 2008; Richardson and others 2006). At the QYZ site, *SWC* has been proven to be a good indicator for maximum carboxylation rate (Ju and others 2010). In addition, Yu and others (2008) have used multiple linear regression with T_a and *SWC* to simulate Q_{10}. In this study, we applied multiple linear regression of meteorological variables to simulate the seasonality of A_m and Q_{10}. Quadratic and interactive terms were included in the regression to capture the potential nonlinear relationships between climatic variables and the parameters. Regression variable selection was based on Bayesian information criterion (BIC, Burnham and Anderson 2002).

First, we considered daily T_a, *VPD*, and *SWC* as the potential explanatory variables for A_m, and T_s, and *VPD* and *SWC* for Q_{10}, according to univariate linear correlation between climatic variables and model parameters. We then constructed a series of candidate models with different combinations of potential explanatory variables and their quadratic and two-order interactive terms. The BIC of each candidate model was calculated by

$$BIC = -2 \times \log(Likelihood) + k \times \log(n), \quad (3)$$

where k is the number of parameters, n is the length of data, and *Likelihood* is the likelihood function. The likelihood function is the probability density function (PDF) of the joint distribution of the model parameters when the data are given. The model with the lowest BIC was selected and then the explanatory variables in this model were used in the next steps. After model selection, the best model for Q_{10} at QYZ was identified as:

$$Q_{10} = a_0 + a_1 \times T_s + a_2 \times SWC + a_3 \times T_s \times SWC \quad (4)$$

and the best model for A_m was

$$A_m = b_0 + b_1 \times T_a + b_2 \times VPD + b_3 \times SWC, \quad (5)$$

where a_i (i = 0, 1, 2, 3) and b_i (i = 0, 1, 2, 3) are parameters. Therefore, we constructed an empirical model for *NEE*, which is expressed as

$$NEE_{predict} = R_{10} Q_{10}^{\frac{T_s - 10}{10}} - \frac{A_m \cdot PAR}{PAR + K_m}, \quad (6)$$

where Q_{10} and A_m are functions of climate variables and R_{10} and K_m are constant parameters.

The parameters of the empirical model were estimated by Bayesian parameterization with the Markov Chain Monte Carlo (MCMC) method (McCarthy 2007) using non-gap filled half-hour data. The posterior probability of a parameter set θ_i could be obtained from

$$\Pr(\theta_i|Data) = \frac{\Pr(\theta_i) \times \Pr(Data|\theta_i)}{\sum_j (\Pr(\theta_i) \times \Pr(Data|\theta_i))}, \quad (7)$$

where $\Pr(\theta_i|Data)$ is the posterior probability of θ_i, which means the joint probability of parameter set θ_i when given the data. $\Pr(\theta_i)$ is the prior probability of θ_i, and $\Pr(Data|\theta_i)$ is the likelihood function. For a normal distribution, the likelihood function is expressed as

$$Likelihood = \prod_{i=1}^{n} \left(\frac{1}{\sqrt{2\pi}\sigma} e^{-\frac{1}{2}\left(\frac{\varepsilon_i}{\sigma}\right)^2} \right), \quad (8)$$

where ε_i is the model residual. When the maximum likelihood method is used to estimate model parameters, the statistics σ can be calculated from the following equation:

$$\sigma^2 = \frac{\sum_{i=1}^{n} \varepsilon_i^2}{n} \quad (9)$$

There are a total of ten parameters to be optimized with uniform prior distributions.

The same approach was applied to MOZ and DK1, but the best models for Q_{10} and A_m at these sites were

$$Q_{10} = a_0 + a_1 \times T_s + a_2 \times SWC + a_3 \times T_s \times SWC$$
$$A_m = b_0 + b_1 \times T_a + b_2 \times VPD + b_3 \times VPD^2 \quad (10)$$

and

$$Q_{10} = a_0 + a_1 \times T_s + a_2 \times SWC + a_3 \times T_s \times SWC$$
$$A_m = b_0 + b_1 \times T_a + b_2 \times VPD + b_3 \times VPD^2 \quad (11)$$

respectively.

Statistical Analysis

At the QYZ site, we ran the models with separate year's data, and obtained seven parameter sets. Following Richardson and others (2007) procedure, we then ran the empirical model by crossing each ''driver year'' with each ''parameters year'' and obtained a 7 × 7 matrix of model predictions. This ''cross model'' was run for 500 iterations. The analysis of variance (ANOVA) with factors of ''driver year,'' ''parameter year,'' ''driver year'' × ''parameter year'' interaction, and ''parameter year'' × ''model run'' interaction was used to partition the total variance of the model predictions. The majority (>95%) of the interannual variation came from the factors ''driver year'' and ''parameter year,'' the contributions to total variation were regarded as the contributions of climatic and biotic effects to the interannual variation in C fluxes, respectively. This approach was applied to model predictions aggregated at daily, weekly, monthly, seasonal, and annual periods, resulting in the contributions of biotic and climatic effects to the IAV of C fluxes at the corresponding periods. To investigate the possible relationship between biotic and climatic effects, the main effects of the factor ''driver year'' and ''parameter year'' were defined as the magnitude of biotic and climatic effects, respectively. The same approach was applied to MOZ and DK1. Following Yuan and others (2009) approach, we used standard deviation to represent the absolute interannual variability (AIAV) and the coefficient of variation (CV) to represent the relative interannual variability (RIAV).

All analyses but Bayesian parameter estimation were applied in R (R Development Core Team 2011), which is a free, open source software environment for statistical computing and graphics with thousands of packages. WinBUGS (version 1.4.3, http://www.mrc-bsu.cam.ac.uk/bugs/) was used to conduct the Bayesian analysis.

Results

Interannual Variability in Climate and Carbon (C) Fluxes

The climatic variables (*PAR*, T_a, T_s, *PPT*, *SWC*, and *VPD*) showed large interannual variability (IAV) at both annual and monthly scales (Figure S1, S2, S3). The relative IAV (RIAV, represented by the coefficient of variation (CV)) in annual *PAR*, *PPT*, and *VPD* was greater than that in T_a, T_s, and *SWC* at QYZ (Figures S1B, D, F), whereas the RIAV in *PPT*, *SWC*, and *VPD* was greater than that in *PAR*, T_a, and T_s at MOZ and DK1 (Figures S2, S3). At the monthly scale, the RIAV in T_a and T_s was lower than that in other climatic variables at all the sites. The variables associated with water conditions (*PPT*, *SWC*, and *VPD*) showed larger IAV in the growing season than other periods (Figures S1, S2, S3). Note that T_a and T_s did not show the same patterns at the annual scale at QYZ ($r^2 = 0.22$, $P > 0.05$) and DK1 ($r^2 = 0.46$, $P > 0.05$), although the seasonality and IAV at the monthly scale were close (Figures S1C, S3C). For the period considered in this study, two extreme climate events occurred at QYZ, a severe summer drought with high temperatures in 2003 and an ice storm event from late January to early February 2008. At MOZ, the precipitation in 2006 and 2007 was lower than that in other years. At DK1, the precipitation in 2007 was the lowest over the period 2003–2007.

During the study period, the annual *NEE* was -333 ± 47 (mean ± SD), -479 ± 65 and 34 ± 92 g C m^{-2} y^{-1} at QYZ (2003–2009), MOZ (2005–2009), and DK1 (2003–2007), respectively (Figure 1B, D, F). At the monthly scale, AIAV of *NEE* was 4–17, 6–58, and 5–41 g C m^{-2} mon^{-1} in QYZ, MOZ, and DK1, respectively. The RIAV in the monthly *NEE* was much larger than that at the annual scale. Although the monthly *NEE* was strongly correlated with the climatic variables, significant correlations were only found between *NEE* and T_s at QYZ ($r^2 = 0.61$, $P < 0.05$) and between *NEE* and *PPT* at DK1 ($r^2 = 0.65$, $P < 0.05$) at the annual scale.

Model Parameters and Performance

The modeled *NEE* at the half-hour, daily, weekly, and monthly scales had good agreement with

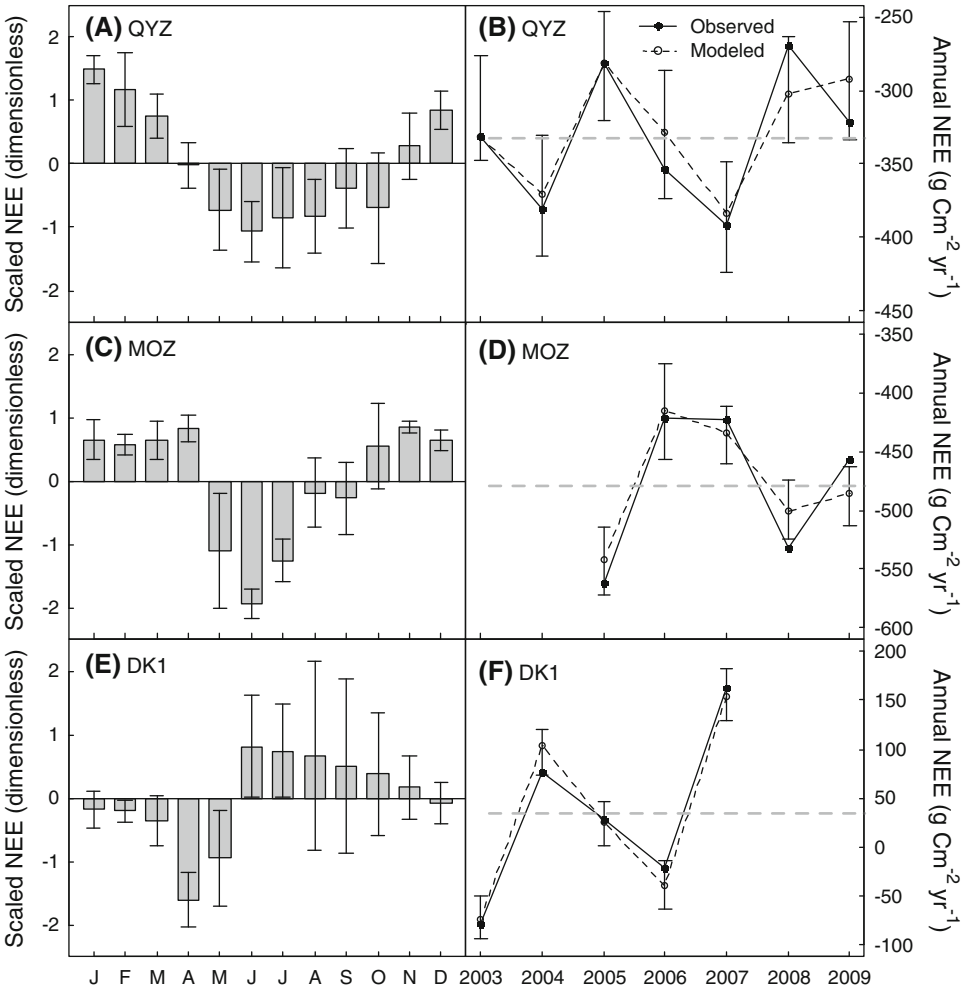

Figure 1. Seasonal (**A**, **C**, **E**) and interannual variability (**B**, **D**, **F**) in *NEE* for the study period at QYZ, MOZ, and DK1. The scaled *NEE* was calculated by $(X_i - \text{mean})/\text{SD}$, where X_i is *NEE* in a specific month during the study period. **B**, **D**, **F** represent observed and modeled annual *NEE*. *Error bars* in modeled values are the range of the 95% credible interval predicted by the empirical model. The *gray dashed horizontal lines* are the means of the observed annual *NEE*.

observed values for all three sites (Figure 2). At the annual scale, the modeled *NEE* was -324 ± 39 (mean $\pm$ SD), -475 ± 51 and 34 ± 95 g C m^{-2} y^{-1} at QYZ, MOZ, and DK1, respectively, closely matching the corresponding observed values in terms of magnitude, RIAV, and interannual patterns ($r^2 = 0.89$, $P < 0.01$; $r^2 = 0.88$, $P < 0.05$; and $r^2 = 0.96$, $P < 0.01$, respectively, Figure 1B, D, F). At QYZ, the model caught the suppression of summer drought on *GPP* and *RE* in 2003, but failed to capture the weak summer suppression in 2004 and 2005 (Figures S6A, S7A). However, the model underestimated the *RE* on cold days with high Q_{10} (Figures 5B, S7A). At the annual scale, the model overestimated *RE* in 2009 and *GPP* in 2008 and 2009 (Figures S4B, S5B). At MOZ, the *NEE* had a clear seasonality, which was well captured by the model. However, the model overestimated both *GPP* and *RE* in 2006 (Figures S4D, S5D) when the temperature was higher and the precipitation was lower than those in the normal years (Figure S2B, D). At DK1, some large model-data mismatching of *NEE* and *GPP* occurred on some days in warmer and drier years (2006 and 2007, Figures 2C, S6C).

Parameterization of the empirical model was conducted yearly during the study period with seven parameter sets for QYZ and five for MOZ and DK1. The PDFs of parameters K_m and R_{10} varied greatly among years at all three sites with larger variation at MOZ and DK1 (Figure 3). Parameter K_m was significantly correlated with annual *PAR* ($r^2 = 0.60$, $P < 0.05$, Figure 4A) and *SWC* ($r^2 = 0.62$, $P < 0.05$, Figure 4B) at QYZ, and with annual *PAR* ($r^2 = 0.80$, $P < 0.05$, Figure 4C) and *PPT* ($r^2 = 0.89$, $P < 0.05$, Figure 4D) at DK1 but not at MOZ as well as R_{10}.

At QYZ, the A_m increased by 0.035 ± 0.0058 mg C m^{-2} s^{-1} (mean $\pm$ SD) with the increment of 1°C in T_a based on the yearly relationship between A_m and T_a during the study period and decreased by 0.48 ± 0.11 mg C m^{-2} s^{-1} with 1 kPa in *VPD*, but the effects of *SWC* on A_m

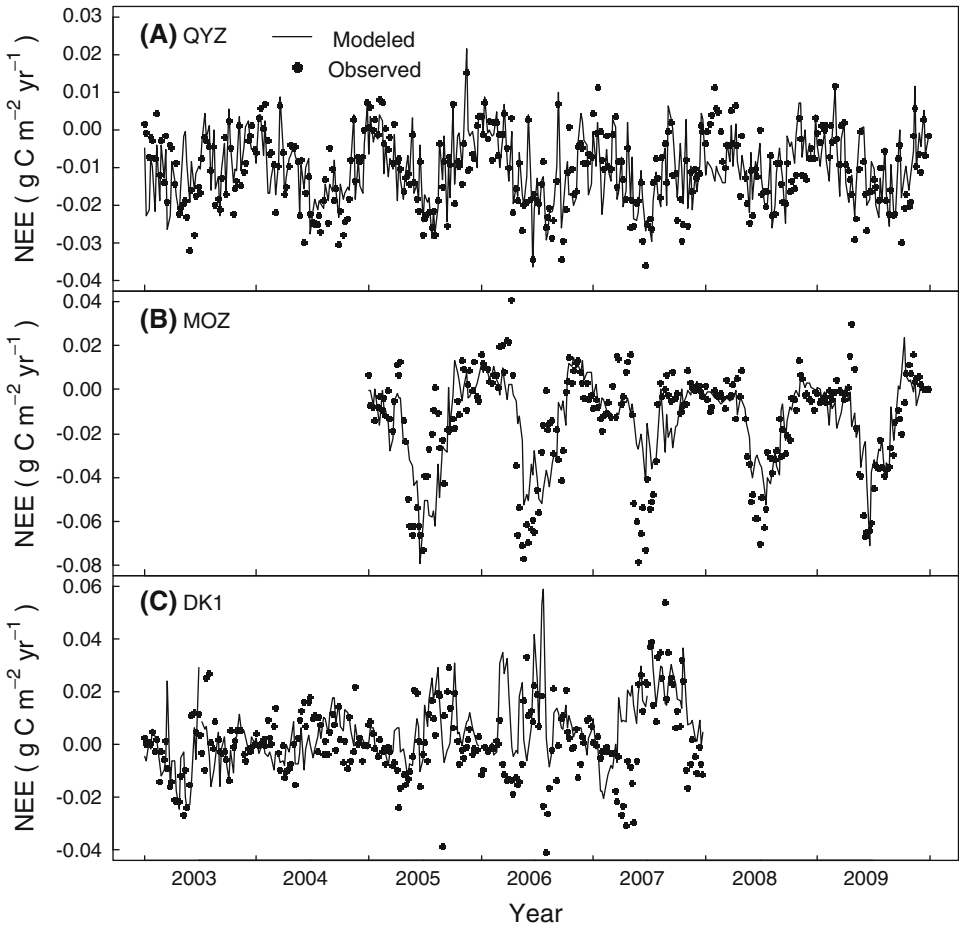

Figure 2. Comparison of modeled and observed *NEE* at QYZ (**A**), MOZ (**B**), and DK1 (**C**) for the study period. The *values* represent the weekly mean *NEE*.

were minor. The maximum A_m was 0.4920 mg C m^{-2} s^{-1} in 2006, whereas severe summer drought resulted in a low A_m in both 2003 and 2007 (Figure 5A). The Q_{10} values decreased with T_s (0.037 ± 0.029 for every 1°C when *SWC* was kept at 30%) and increased with *SWC* (0.042 ± 0.038 for every percent of *SWC* when T_s was kept at 18°C). The mean Q_{10} in a calendar year ranged from 1.9 to 2.7, and the Q_{10} pattern was different among years (Figure 5B). For example, the Q_{10} values declined from 3.5 to 2.0, and then increased to the former level in 2005 and 2007, whereas it declined from 4.5 to 1.2 during the whole year in 2003 (Figure 5B), which might have resulted mainly from the continuously declining *SWC* due to severe drought (r^2 = 0.41, $P < 0.001$). In 2009, the Q_{10} values remained relatively unchanged within 1.6–2.1 (Figure 5B), probably due to the relative low variations of *SWC*.

The relationships between daily A_m and climatic variables T_a and *VPD* at MOZ were nonlinear and varied among years. However, the A_m reached the maximum when T_a was about 24°C and *VPD* about 1 kPa. The Q_{10} values deceased by 0.052 ± 0.049 with the increment of 1°C in T_a and increased by 0.038 ± 0.028 with 1% in *SWC*. At DK1, the daily A_m increased with T_a (0.0062 ± 0.0032 mg C m^{-2} s^{-1} for 1°C), and reached the maximum when *VPD* was about 1 kPa. However, the relationships between Q_{10} and climatic variables T_s (−0.056 to 0.049 for 1°C increment when *SWC* kept at 30%) and *SWC* (−0.0056 to 0.049 for 1% increment when T_s kept at 16°C) were not consistent among years.

Climatic and Biotic Effects on C Fluxes

The contributions of climatic effects to the IAV in C fluxes decreased when the temporal scale increased from days to years for all three sites (Figure 6A, C, E) with a larger contribution in the forests (QYZ and MOZ) than in the grassland (DK1). At QYZ, the contribution of climatic effects to the IAV in *NEE* was closer to that in *GPP* than *RE* (Figure 6A), whereas DK1 had the opposite pattern (Figure 6E). At MOZ, the contributions of climatic effects were similar for *NEE*, *GPP*, and *RE* (Figure 6C). At all

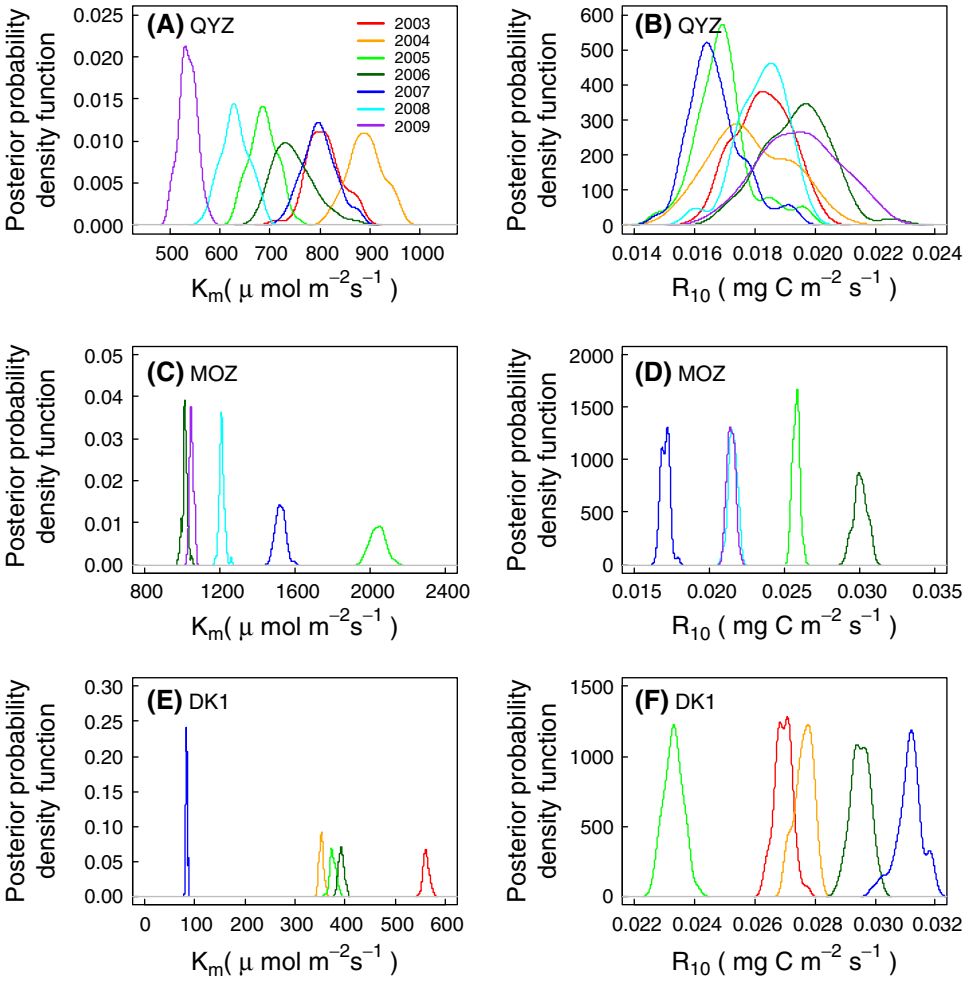

Figure 3. Posterior probability distribution functions (PPDF) of parameters K_m (**A**, **C**, **E**) and R_{10} (**B**, **D**, **F**) at QYZ, MOZ, and DK1. The *area below each curve* is 1. At QYZ, the distribution of K_m in 2003 and 2007 was not significantly different, the distribution of R_{10} in 2008 was not significantly different from those in 2003 and 2004. At MOZ, the distribution of R_{10} in 2008 and 2009 was not significantly different. Others are all significantly different for K_m and R_{10} at the three sites.

three ecosystems, the contributions of climatic effects to the IAV in *NEE* were lower in the growing season than the non-growing season (Figures 7, S10, S11). The magnitude of climatic effects on annual *NEE* at QYZ, MOZ, and DK1 ranged from −131 to 127, from −73 to 107, and from −60 to 89 g C m^{-2} y^{-1}, respectively (Figure 8A–C). Annual *PAR*, *SWC*, and *VPD* all were correlated with climatic effects on *NEE* at QYZ (Table 1). The climatic effects on *NEE* were correlated with annual *PAR* in MOZ and annual *VPD* in DK1 (Table 1).

On the contrary, the contributions of biotic effects increased when the temporal scale increased from days to years (Figure 6B, D, F). The magnitude of biotic effects on annual *NEE* at QYZ, MOZ, and DK1 were from −95 to 170, from −99 to 78, and from −204 to 318 g C m^{-2} y^{-1}, respectively (Figure 8A–C). Interestingly, we found a significant negative correlation between climatic and biotic effects on *NEE* ($r^2 = 0.80$, $P < 0.01$) and *GPP* ($r^2 = 0.61$, $P < 0.05$) at the annual scale at QYZ (Figure 8J) but not at the other two sites.

Discussion

Climatic and Biotic Drivers of the IAV in *NEE*

Quantifying net ecosystem exchange of CO_2 (*NEE*) and its components (*GPP* and *RE*) and identifying its controlling drivers is critical for understanding ecosystem functioning and global C cycling. In this study, we partitioned the IAV in C fluxes into climatic and biotic effects, and quantified the relative contributions of these two effects. At QYZ, the relative contribution of climatic and biotic effects to the IAV in *NEE* was closer to that in *GPP* compared to *RE*, whereas the pattern was the opposite at DK1. At MOZ, *GPP* and *RE* were similar to *NEE* in terms of climatic and biotic effects (Figure 6). Yuan and others (2009) defined the C uptake period as the continuous period when a 5-day running average of *NEE* was negative and suggested that the longer the C sink period, the more important *GPP* (and less importance of *RE*) was to *NEE*, because *GPP* was the dominant flux in the C sink period

whereas *RE* drove the variation of *NEE* during the dormancy period of plants. Our results confirmed this idea, which showed that the C sink periods were 298, 254, and 183 days at QYZ, MOZ, and DK1, respectively.

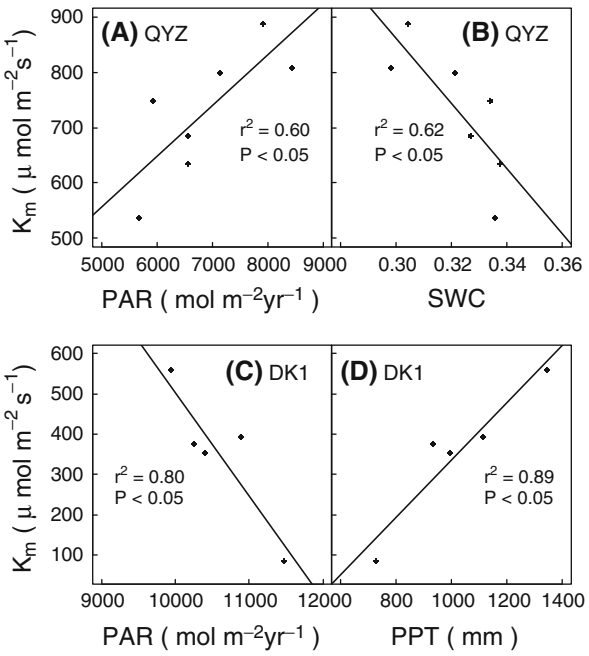

Figure 4. Linear relationships between parameter K_m and annual mean climatic variables at QYZ (**A**, **B**) and DK1 (**C**, **D**). There were no other significant relationships of K_m and R_{10} with other climatic variables for all three sites.

Annual *NEE* was usually linearly related to annual solar radiation, air or soil temperature, and water conditions (Archibald and others 2009; Pintér and others 2008; Wen and others 2010) as well as climatic factors in specific month(s) (Allard and others 2008; Zhang and others 2011a) and climatic events such as severe drought and El Niños (Aires and others 2008; Wharton and others 2009). However, the simple correlations between annual *NEE* and climatic variables above might confound the underlying mechanisms of IAV in *NEE*, because climatic effects on IAV in *NEE* were different from annual *NEE*. For example, although annual *NEE* was significantly correlated with T_s at QYZ ($r^2 = 0.61$, $P < 0.05$), the modeling results showed that radiation and water conditions, rather than temperature, were the main climatic drivers on IAV (Table 1). At MOZ and DK1, the primary climatic drivers of IAV in *NEE* were radiation and water conditions, respectively (Table 1). The warm climate of the three sites indicated that the temperature did not constrain the C fluxes, whereas the relatively dry summer made water conditions a primary controller of *NEE* at QYZ and DK1. Radiation might affect *NEE* at QYZ via light supply, change in evapotranspiration, and photoinhibition. At MOZ, there was no strong constraint of water conditions on *NEE* due to the year-round humid climate, resulting in the dominant effect of radiation.

IAV in *NEE* was also affected by biotic drivers such as maximum photosynthetic rate (A_m) and reference respiration rate (R_{10}, Humphreys and Lafleur 2011), which contributed to biotic effects.

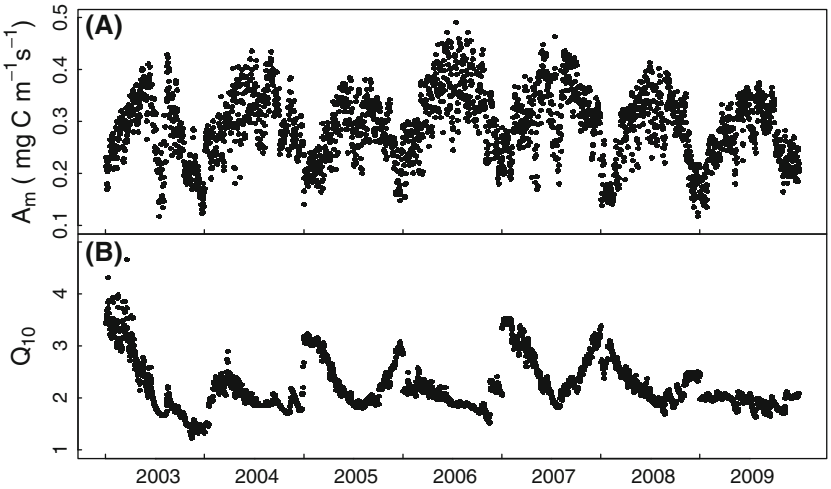

Figure 5. Daily A_m (**A**) and Q_{10} (**B**) from 2003 to 2009 at QYZ. The values were obtained from the equations $A_m = b_0 + b_1 \times T_a + b_2 \times VPD + b_3 \times SWC$ and $Q_{10} = a_0 + a_1 \times T_s + a_2 \times SWC + a_3 \times T_s \times SWC$ using the values of parameters from the parameterization of the empirical model. Daily A_m and Q_{10} in the other two ecosystems are shown in Supplementary material.

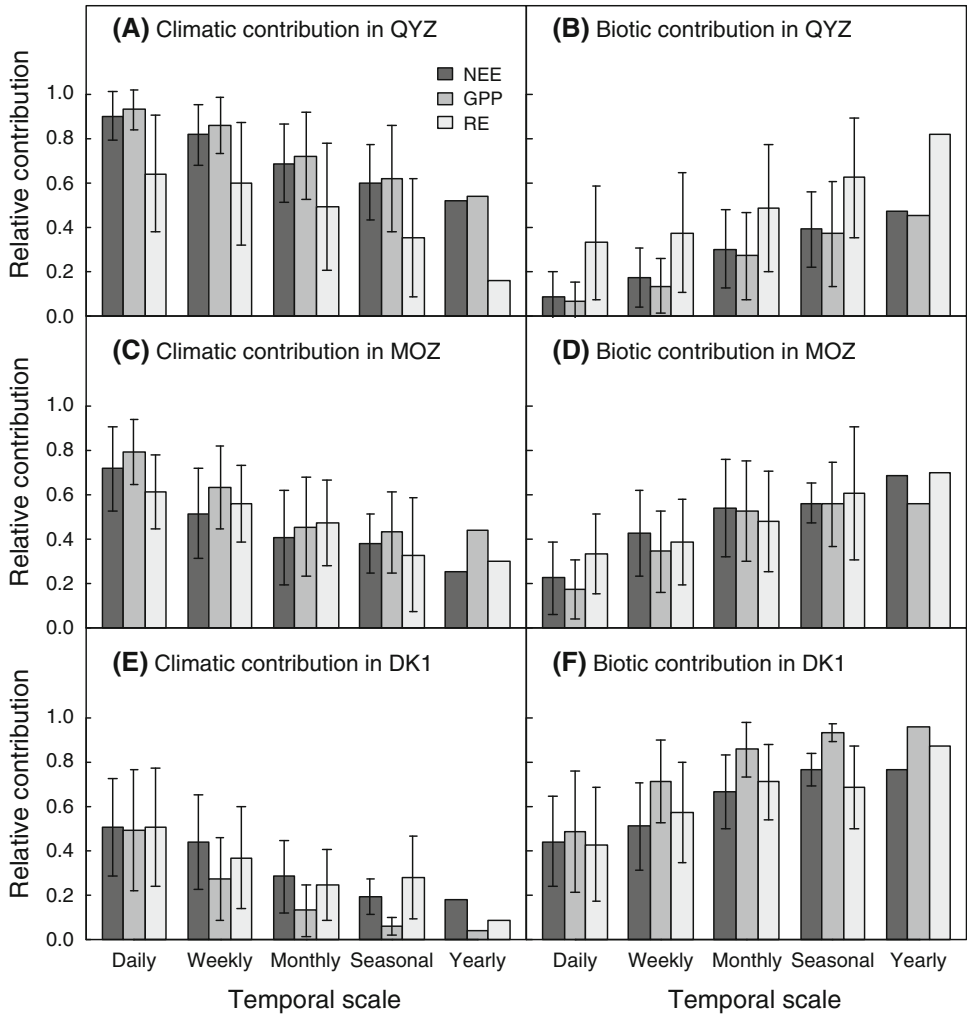

Figure 6. The relative contribution of climatic (**A**, **C**, **E**) and biotic effects (**B**, **D**, **F**) to IAV in fluxes of QYZ, MOZ, and DK1 at the temporal scales from daily to yearly. The *error bars* represent the SD of a certain contribution at the specific scale across the whole period of year.

At all three sites, we found significant changes in A_m, the Michaelis constant (K_m), R_{10} and Q_{10} (Figures 3, 5, S8, S9) among the years as well as in other studies (Richardson and others 2007; Adkinson and others 2011). IAV in biotic drivers may mainly result in biotic effects on IAV in both annual *GPP* and *RE*. Because IAV in *NEE* was controlled by different fluxes (*GPP* or/and *RE*) among the three ecosystems, the main biotic drivers of annual *NEE* also differed from photosynthetic (A_m and K_m) to respiratory capacities (Q_{10} and R_{10}). However, it is difficult to identify one or two primary biotic drivers due to complex interactions and the limited data.

Climatic and Biotic Effects on IAV in *NEE*

Variations in climatic variables (diel and seasonality) drive short-term variability in C fluxes, whereas biotic drivers may be more important at the long-term scale (Baldocchi 2008; Luo and Weng 2011). Our results showed that the contributions of biotic effects to variations in C fluxes become more important with the increasing temporal scale from days to years in spite of different vegetation types (Figure 6, Richardson and others 2007; Wu and others 2012). Temporally, the contributions of biotic effects were larger in the growing season than the non-growing season within a year (Figures 7, S10, S11), which was consistent with our definition of biotic effects as the result of IAV in plant physiological activities. Spatially, it was suggested that the biotic effects were more important in deciduous than evergreen vegetation for both forests and wetlands (Adkinson and others 2011; Richardson and others 2007; Wu and others 2012) and more important in grasslands than forests (Polley and others 2008), because the former was more sensitive to climate variation (Adkinson and others 2011; Wu and others 2012). In this study, we also found that the contribution of biotic effect to IAV in *NEE* at the annual scale was the largest in the grassland (DK1, 77%), followed by the deciduous (MOZ, 69%) and evergreen for-

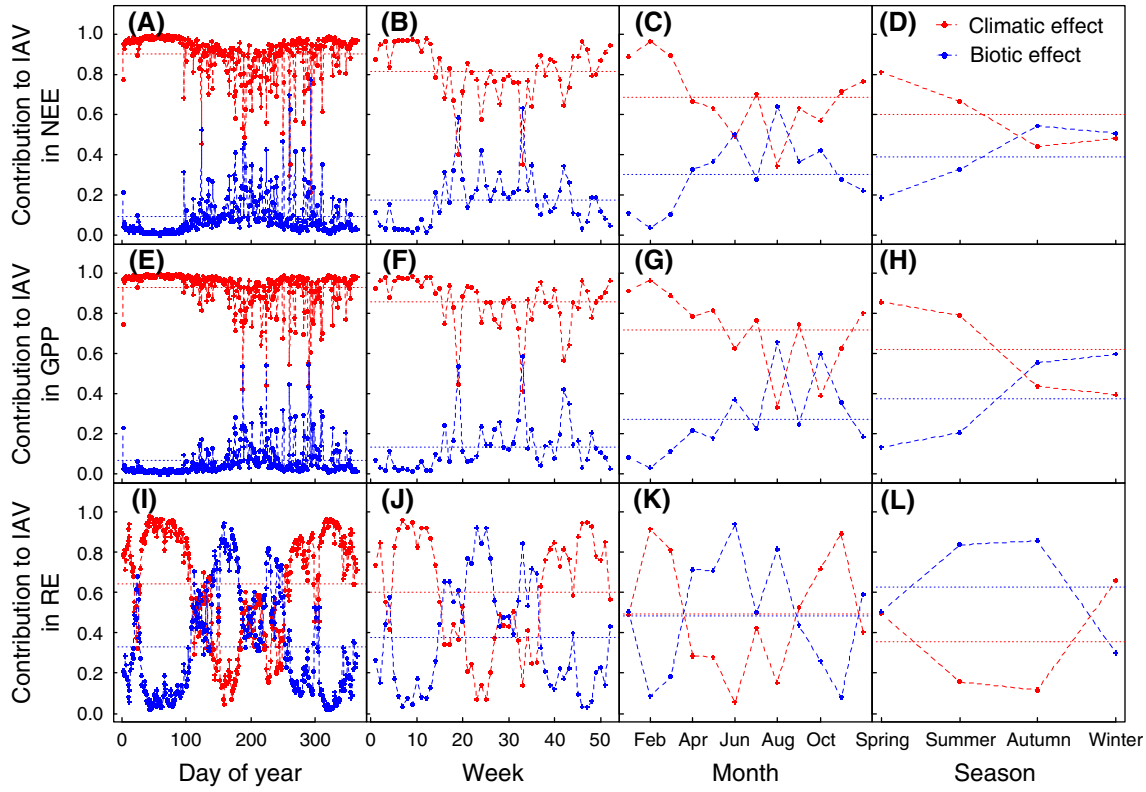

Figure 7. Contributions of climatic and biotic effects to interannual variability in *NEE* (**A–D**), *GPP* (**E–H**), and *RE* (**I–L**) at daily, weekly, monthly, and seasonal scales at QYZ. The values were derived by partitioning the variance by analysis of variance (ANOVA) in crossed model predictions at the specific day (or week, month, season) of the year. Those for the other two ecosystems are shown in Supplementary material.

ests (QYZ, 47%). However, whether the vegetation type is the primary factor controlling the relative contribution of biotic effects is still unclear.

Interestingly, we found a strong negative correlation between the climatic and biotic effects on both annual *NEE* and *GPP* (Figure 8J) at QYZ, compared to a weak non-significant correlation in Howland Forest (Richardson and others 2007), MOZ and DK1 (Figure 8K, L). Because the responses of ecosystem C fluxes to climatic change can be partitioned into climatic and biotic effects with the opposite directions, the combined effect (climatic + biotic effects) at QYZ may not fluctuate dramatically. Therefore, the QYZ plantation has robust ecosystem functioning in terms of C cycling, in spite of the variations of climatic variables. For example, the climatic effect caused the plantation to absorb less C from 2003 to 2009 with a decrease of 36.2 g C m^{-2} y^{-1}, whereas the biotic effect offset the climatic one to a large degree (Figure 8A, J).

The relatively stable C sink may result from ecological resistance to climatic variability for several reasons. First, the ecological and biological properties of the dominant species *P. massoniana* and *P. elliottii*, with the waxy structures on the leaves and associating mycorrhizal fungi, may enhance water availability and water use efficiency and then reduce evapotranspiration (Wang and Ding 2013; Zhang and others 1999). The subtropical evergreen plantation may thus be drought resistant and has the ability to reduce the stress of water deficit. Second, although the summer drought suppressed both *GPP* and *RE*, there was usually sufficient water during the pre-summer period (data not shown), which might stimulate microorganism activity, increase nutrient availability (Brooker 2006), and thus ameliorate environmental limitations to the biotic effects.

At all three sites, the IAV in radiation and water conditions was greater than that in temperature. However, how these climatic variables directly and indirectly affect C fluxes are crucial to understand the underlying mechanisms of response of ecosystem C cycling to climatic change. At QYZ, the model parameter K_m was strongly positively correlated with annual *PAR* and negatively with *SWC* ($r^2 > 0.60$, $P < 0.05$, Figure 4A, B). Because the annual mean A_m was not correlated with annual

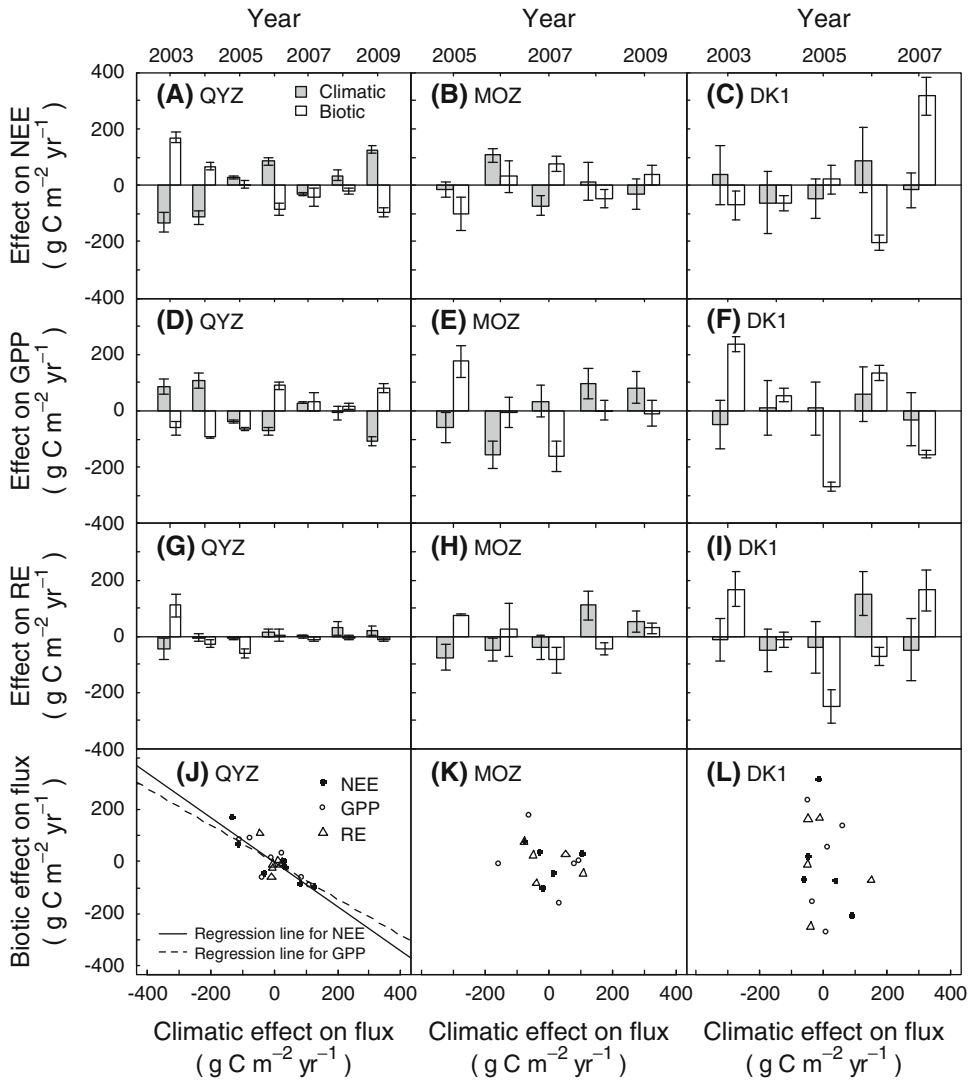

Figure 8. Climatic and biotic effects on *NEE* (**A**–**C**), *GPP* (**D**–**F**), and *RE* (**G**–**I**) at the annual scale, and their relationship between the two effects (**J**–**L**) in QYZ, MOZ, and DK1. The values were calculated as the difference between the estimated value of climatic (or biotic) effect in the specific year and the mean across 7 years. The *error bars* represent standard deviation for the study period. Linear relationships between climatic and biotic effects in **J** were significant for *NEE* ($r^2 = 0.80$, $P < 0.01$) and *GPP* ($r^2 = 0.61$, $P < 0.05$).

Table 1. Correlation Coefficients (r) Between Annual Climatic Variables and Climatic (or Biotic) Effects on IAV in Annual *NEE* at QYZ, MOZ, and DK1

r	QYZ		MOZ		DK1	
	$NEE_{climatic}$	NEE_{biotic}	$NEE_{climatic}$	NEE_{biotic}	$NEE_{climatic}$	NEE_{biotic}
PAR	−0.99*	0.93*	−0.97*	0.78	0.39	0.66
T_a	−0.42	0.29	0.58	−0.13	0.70	0.46
T_s	−0.50	0.29	0.46	−0.29	0.59	0.35
PPT	0.16	−0.33	−0.53	−0.03	−0.47	−0.83*
SWC	0.94*	−0.90*	−0.65	0.43	−0.28	−0.73
VPD	−0.80*	0.86*	0.56	−0.15	0.80*	0.31

*$P < 0.05$.

PAR or *SWC* (both $P > 0.9$) at QYZ, the maximum photosynthetic rate was more difficult to reach if the K_m was the larger. Thus, the positive correlation between *PAR* and K_m indicated that the direct and indirect effects of *PAR* on *GPP* were opposite based on the light compensation curve (Falge and others 2001), whereas the direct and indirect effects of *SWC* were consistent due to the negative

correlation between *SWC* and K_m. On the contrary, K_m was strongly negatively correlated with annual *PAR* and positively to *PPT* ($r^2 > 0.80$, $P < 0.05$, Figure 4C, D) at DK1. The annual mean A_m was positively correlated with K_m and *PPT* ($r^2 = 0.80$, $P < 0.05$) and negatively to *PAR* ($r^2 = 0.46$, $P = 0.21$), resulting in the opposite direct and indirect effects of *PAR* through K_m and A_m on *GPP* and similar effects of *PPT*. However, it is difficult to partition the effects of *PAR* and water conditions on photosynthetic capacity due to the high correlation between them at the annual scale, and the ultimate relationships between the indirect and indirect effects of climate depend on the relative importance of these climatic variables to *GPP*.

The previous and current studies found that the seasonality of A_m and Q_{10} was correlated with temperature and water conditions (Ju and others 2010; Ricciuto and others 2008; Yu and others 2008). At QYZ, the positive effect of T_a on A_m was usually greater than the negative effect of *VPD*, whereas in the severe drought summer, the negative effect of *VPD* dominated and then suppressed A_m, especially in 2003 (Figure 5A). At MOZ and DK1, the effects of T_a and *VPD* on A_m were similar to those at QYZ, except that there was no strong summer suppression on A_m (Figures S8A, S9A). At QYZ and MOZ, the temperature sensitivity of *RE* (Q_{10}) decreased with T_s and increased with *SWC*. When *SWC* was kept constant at an average level of 30%, Q_{10} values decreased 0.037 ± 0.029 and 0.052 ± 0.049 with every 1°C in T_s at QYZ and MOZ, respectively, which was similar to the average value of 0.046 ± 0.0033 for foliage respiration from 56 species in arctic, boreal, temperate, and tropical biomes (Tjoelker and others 2001). The dependence of Q_{10} on temperature was usually attributed to the acclimatization of respiration (Luo and others 2001). However, a recent study has found that Q_{10} values of *RE* did not differ among biomes at a global scale, being independent of temperature (Mahecha and others 2010). The results from DK1 showed that the effects of 1°C increment in T_s on Q_{10} varied from −0.056 to 0.049 due to a complex interactions between temperature and water conditions. The different effects of temperature on Q_{10} values might have resulted from the influence of the confounding factors as well as methods and scales.

Model Performance, Limitations, and Implications

In our study, the empirical model captured both the seasonality and IAV in *NEE* relatively well, with good agreement between the observations and modeled results both in terms of AIAV and RIAV (Figure 1; ''Interannual Variability in Climate and Carbon (C) Fluxes'' and ''Model Parameters and Performance'' sections). For example, the observed *NEE* was very close to the simulated annual *NEE* (-333 ± 47 vs. -324 ± 39 g C m^{-2} y^{-1}) within the range of −197 to −430 g C m^{-2} y^{-1} in previous studies at QYZ (Yu and others 2008; Liu and others 2009; Wen and others 2010; Zhang and others 2011b). Nevertheless, systematic and random errors may challenge the reliability of estimated annual fluxes and their IAV (Mauder and others 2013). Fortunately, standardized data-processing approaches considerably reduce the systematic error to typically 5–10% and have little effect on the IAV (Baldocchi 2008). The aggregated random error on the annual scale is generally about 5% (Baldocchi 2008), and compared to the much larger IAV in *NEE*, this level of error may not significantly affect our results (Mauder and others 2013; Stoy and others 2008).

The plantation experienced a severe drought in 2003 at QYZ, becoming a C source in the summer, but it was still a strong C sink over the whole year comparable to normal years. This is because the ecosystem has higher C uptake before the drought due to the sufficient supply of soil water (Wen and others 2010). In early 2008, a strong ice storm caused great biomass losses (227 g C m^{-2}), resulting in lower C uptake than that in normal years due to the large reduction in *GPP* (Zhang and others 2011b). Usually, such extreme climatic events increase uncertainties in simulating C fluxes (Ju and others 2010). The water deficiency and heat stress usually suppress both *GPP* and *RE*, and in most cases the response of *GPP* is more dramatic than that of *RE* (Schwalm and others 2010). At QYZ, the severe drought in 2003 and 2007 considerably decreased C fluxes in summer, which was difficult to simulate in the empirical and/or mechanistic models (Ju and others 2010). The extreme drought in the summer of 2003 thus resulted in a larger disagreement between modeled and observed daily *NEE* ($r^2 = 0.54$, $P < 0.001$) compared to the normal condition ($r^2 = 0.70$, $P < 0.001$, Figure 2A). Such an effect of drought on model performance also occurred for *NEE* in 2006 and 2007 at MOZ (Figure 2B). At QYZ, the severe ice storm in early 2008 caused both physical damage and physiological injury (Ma and others 2010; Zhang and others 2011b). The physical damage resulted in the loss of 200 and 2,206 g C m^{-2} in branch breakage area and severely damaged area, respectively (Ma and others 2010). Although the

empirical model was able to capture the IAV by changing the parameters, it seemed not to be as flexible as the gap-filling model to capture the sudden large loss of photosynthetic tissues, resulting in overestimated annual *GPP* in 2008 and 2009 and overestimated annual *RE* in 2009.

The difference between modeled and observed *NEE* at QYZ mainly resulted from the difficulties in simulating *RE*, which might be the result of low correlations between nighttime F_c and climatic variables ($r^2 = 0.32$, $P < 0.001$ for half-hour scale) and the extensive gaps due to unrealistic conditions. The poor model performance also resulted in a large contribution of the biotic effect on *RE* (Figure 7I–L). At MOZ, similar model errors were also found for *RE* in 2005 and 2006 when the precipitation was low and the temperature was high (Figure S7B). Although some studies suggested that those models with *GPP* as biotic drivers could better simulate the dynamics of *RE* (Kuzyakov and Gavarichkova 2010; Migliavacca and others 2011), the problem of simulating *RE* was still pervasive (Mitchell and others 2011). Time lag between *GPP* and *RE* (Kuzyakov and Gavarichkova 2010; Vargas and others 2011) and the lack of other biotic data (for example, soil C pool) might have influenced model performance. Moreover, we found that the effect of *SWC* on Q_{10} decreased with temperature at QYZ, which may not be suitable for severe drought situations, in which high temperature accelerates the negative effect of water stress. This causes additional difficulties in simulating IAV in C fluxes.

Understanding the underlying mechanisms of IAV in C fluxes is important for developing ecological theories and projecting future ecosystem changes (Hui and others 2003). Our study highlights the necessity of partitioning IAV in C fluxes into climatic and biotic effects, because the current process-based models generally failed to reproduce the interannual dynamics of C fluxes (Keenan and others 2012). Process-based mechanistic models would be more robust for predicting IAV in C fluxes if the biotic effects are incorporated into the model at annual and longer time scales. Moreover, it is difficult for both statistical and mechanistic models to simulate the sudden and dramatic effects of extreme events on C fluxes, which need to receive more attention in climate-impact research (Reichstein and others 2013).

ACKNOWLEDGMENTS

The authors thank the two anonymous reviewers for their insightful comments and suggestions. This research was financially supported by the National Basic Research Program of China (2010CB833504), the National Natural Science Foundation of China (31070407, 31370489), 2012 Shanghai Pujiang Program (12PJ1401400), ''Thousand Young Talents'' Program in China, and The Program for Professor of Special Appointment (Eastern Scholar) at Shanghai Institutions of Higher Learning.

REFERENCES

Adkinson AC, Syed KH, Flanagan LB. 2011. Contrasting responses of growing season ecosystem CO_2 exchange to variation in temperature and water table depth in two peatlands in northern Alberta. Can J Geophys Res 116:G01004.

Aires LMI, Pio CA, Pereira JS. 2008. Carbon dioxide exchange above a Mediterranean C3/C4 grassland during two climatologically contrasting years. Glob Change Biol 14:539–55.

Allard V, Ourcival JM, Rambal S, Joffre R, Rocheteau A. 2008. Seasonal and annual variation of carbon exchange in an evergreen Mediterranean forest in southern France. Glob Change Biol 14:714–25.

Archibald SA, Kirton A, van der Merwe MR, Scholes RJ, Williams CA, Hanan N. 2009. Drivers of inter-annual variability in net ecosystem exchange in a semi-arid savanna ecosystem, South Africa. Biogeosciences 6:251–66.

Baldocchi D. 2008. Breathing of the terrestrial biosphere: lessons learned from a global network of carbon dioxide flux measurement systems. Aust J Bot 56:1–26.

Baldocchi D, Falge E, Gu L, Olson R, Hollinger D, Running S, Anthoni P, Bernhofer CH, Davis K, Evans R, Fuentes J, Goldstein A, Katul G, Law B, Lee X, Malhi Y, Meyers T, Munger W, Oechel W, Paw UKT, Pilegaard K, Schmid HP, Valentini R, Verma S, Vesala T, Wilson K, Wofsy S. 2001. FLUXNET: a new tool to study the temporal and spatial variability of ecosystem-scale carbon dioxide, water vapor, and energy flux densities. Bull Am Meteorol Soc 82:2415–34.

Barr AG, Black TA, Hogg EH, Griffis TJ, Morgenstern K, Kljun N, Theede A, Nesic Z. 2007. Climatic controls on the carbon and water balances of a boreal aspen forest, 1994–2003. Glob Change Biol 13:561–76.

Brooker RW. 2006. Plant–plant interactions and environmental change. New Phytol 171:271–84.

Buchmann N, Schulze E-D. 1999. Net CO_2 and H_2O fluxes of terrestrial ecosystems. Glob Biogeochem Cycles 13:751–60.

Burnham KP, Anderson DR. 2002. Model selection and multimodel inference. New York: Springer.

Canadell JG, Le Quere C, Raupach MR, Field CB, Buitenhuis ET, Ciais P, Conway TJ, Gillett NP, Houghton RA, Marland G. 2007. Contributions to accelerating atmospheric CO_2 growth from economic activity, carbon intensity, and efficiency of natural sinks. Proc Natl Acad Sci USA 104:18866–70.

Carle J, Holmgren P. 2008. Wood from planted forests: a global outlook 2005–2030. For Prod J 58:6–18.

Cox PM, Betts RA, Jones CD, Spall SA, Totterdell IJ. 2000. Acceleration of global warming due to carbon-cycle feedbacks in a coupled climate model. Nature 408:184–7.

de Beeck MO, Gielen B, Jonckheere I, Samson R, Janssens IA, Ceulemans R. 2010. Needle age-related and seasonal photosynthetic capacity variation is negligible for modeling yearly gas exchange of a sparse temperate Scots pine forest. Biogeosciences 7:199–215.

Dragoni D, Schmid HP, Wayson CA, Potter H, Grimmond CSB, Randolph JC. 2011. Evidence of increased net ecosystem productivity associated with a longer vegetated season in a deciduous forest in south-central Indiana, USA. Glob Change Biol 17:886–97.

Falge E, Baldocchi D, Olson R, Anthoni P, Aubinet M, Bernhofer C, Burba G, Ceulemans R, Clement R, Dolman H, Granier A, Gross P, Grünwald T, Hollinger D, Jensen N-O, Katul G, Keronen P, Kowalski A, Lai CT, Law BE, Meyers T, Moncrieff J, Moors E, Munger JW, Pilegaard K, Rannik Ü, Rebmann C, Suyker A, Tenhunen J, Tu K, Verma S, Vesala T, Wilson K, Wofsy S. 2001. Gap filling strategies for defensible annual sums of net ecosystem exchange. Agric For Meteorol 107: 43–69.

FAO. 2007. State of the World's Forests. Rome, Italy: Food and Agriculture Organization of the United Nations.

Goulden ML, Munger JW, Fan SM, Daube BC, Wofsy SC. 1996. Exchange of carbon dioxide by a deciduous forest: response to interannual climate variability. Science 271:1576–8.

He H, Liu M, Sun X, Zhang L, Luo Y, Wang H, Han S, Zhao X, Shi P, Wang Y, Ouyang Z, Yu G. 2010. Uncertainty analysis of eddy flux measurements in typical ecosystems of ChinaFLUX. Ecol Inform 5:492–502.

Huang M, Ji J, Li K, Liu Y, Yang F, Tao B. 2007. The ecosystem carbon accumulation after conversion of grasslands to pine plantations in subtropical red soil of South China. Tellus 59B:439–48.

Huang L, Liu J, Shao Q, Xu X. 2012. Carbon sequestration by forestation across China: past, present, and future. Renew Sust Energy Rev 16:1291–9.

Hui D, Luo Y, Katul G. 2003. Partitioning interannual variability in net ecosystem exchange between climatic variability and functional change. Tree Physiol 23:433–42.

Humphreys ER, Lafleur PM. 2011. Does earlier snowmelt lead to greater CO_2 sequestration in two low Arctic tundra ecosystems? Geophys Res Lett 38:L09703.

IPCC. 2007. Climate Change 2007: The physical science basis. Cambridge: Cambridge University Press.

Ju W, Wang S, Yu G, Zhou Y, Wang H. 2010. Modeling the impact of drought on canopy carbon and water fluxes for a subtropical evergreen coniferous plantation in southern China through parameter optimization using an ensemble Kalman filter. Biogeosciences 7:845–57.

Keenan TF, Baker I, Barr A, Ciais P, Davis K, Dietze M, Dragoni D, Gough CM, Grant R, Hollinger D, Hufkens K, Poulter B, McCaughey H, Raczka B, Ryu Y, Schaefer K, Tian H, Verbeeck H, Zhao M, Richardson AD. 2012. Terrestrial biosphere model performance for inter-annual variability of land-atmosphere CO_2 exchange. Glob Change Biol 18:1971–87.

Kuzyakov Y, Gavrichkova O. 2010. Time lag between photosynthesis and carbon dioxide efflux from soil: a review of mechanisms and controls. Glob Change Biol 16:3386–406.

Liao CZ, Luo YQ, Fang CM, Chen JK, Li B. 2012. The effects of plantation practice on soil properties based on the comparison between natural and planted forests: a meta-analysis. Glob Ecol Biogeogr 21:318–27.

Liu M, He H, Yu G, Luo Y, Sun X, Wang H. 2009. Uncertainty analysis of CO_2 flux components in subtropical evergreeen coniferous plantation. Sci China Ser D Earth Sci 52:257–68.

Luo Y, Weng E. 2011. Dynamic disequilibrium of the terrestrial carbon cycle under global change. Trends Ecol Evol 26:96–104.

Luo Y, Wan S, Hui D, Wallace LL. 2001. Acclimatization of soil respiration to warming in a tall grass prairie. Nature 413: 622–5.

Luo Y, Sherry R, Zhou X, Wan S. 2009. Terrestrial carbon-cycle feedback to climate warming: experimental evidence on plant regulation and impacts of biofuel feedstock harvest. Glob Change Biol Bioenergy 1:14–29.

Ma Z, Wang H, Wang S, Li Q, Wang Y, Wang H. 2010. Impact of a severe ice storm on subtropical plantations at Qianyanzhou, Jiangxi, China. Chin J Plant Ecol 34:204–12.

Mahecha MD, Reichstein M, Carvalhais N, Lasslop G, Lange H, Seneviratne SI, Vargas R, Ammann C, Arain MA, Cescatti A, Janssens IA, Migliavacca M, Montagnani L, Richardson AD. 2010. Global convergence in the temperature sensitivity of respiration at ecosystem level. Science 329:838–40.

Mauder M, Cuntz M, Drüe C, Graf A, Rebmann C, Schmid HP, Schmidt M, Steinbrecher R. 2013. A strategy for quality and uncertainty assessment of long-term eddy-covariance measurements. Agric For Meteorol 169:122–35.

McCarthy MA. 2007. Bayesian methods for ecology. New York: Cambridge University Press.

Migliavacca M, Reichstein M, Richardson AD, Colombo R, Sutton MA, Lasslop G, Tomelleri E, Wohlfahrt G, Carvalhais N, Cescatti A, Mahecha MD, Montagnani L, Papale D, Zaehle S, Arain A, Arneth A, Black TA, Carrara A, Dore S, Gianelle D, Helfter C, Hollinger D, Kutsch WL, Lafleur PM, Nouvellon Y, Rebmann C, Rocha HR, Rodeghiero M, Roupsard O, Sebastià M, Seufert G, Soussana J, van der Molen MK. 2011. Semi-empirical modeling of abiotic and biotic factors controlling ecosystem respiration across eddy covariance sites. Glob Change Biol 17:390–409.

Mitchell S, Beven K, Freer J, Law B. 2011. Processes influencing model-data mismatch in drought-stressed, fire-disturbed eddy flux sites. J Geophys Res 116:G02008.

Pan Y, Birdsey RA, Fang J, Houghton R, Kauppi PE, Kurz WA, Phillips OL, Shvidenko A, Lewis SL, Canadell JG, Ciais P, Jackson RB, Pacala SW, McGuire AD, Piao S, Rautiainen A, Sitch S, Hayes D. 2011. A large and persistent carbon sink in the world's forests. Science 333:988–93.

Papale D, Reichstein M, Aubinet M, Canfora E, Bernhofer C, Kutsch W, Longdoz B, Rambal S, Valentini R, Vesala T, Yakir D. 2006. Towards a standardized processing of net ecosystem exchange measured with eddy covariance technique: algorithms and uncertainty estimation. Biogeosciences 3:571–83.

Pintér K, Barcza Z, Balogh J, Czobel S, Csintalan Z, Tuba Z, Nagy ZZ. 2008. Interannual variability of grasslands' carbon balance depends on soil type. Commun Ecol 9:43–8.

Polley HW, Frank AB, Sanabria J, Phillips RL. 2008. Interannual variability in carbon dioxide fluxes and flux-climate relationships on grazed and ungrazed northern mixed-grass prairie. Glob Change Biol 14:1620–32.

R Development Core Team. 2011. R: a language and environment for statistical computing. Vienna, Austria: R Foundation for Statistical Computing. ISBN 3-900051-07-0. http://www.R-project.org/.

Reichstein M, Falge E, Baldocchi D, Papale D, Aubinet M, Berbigier P, Bernhofer C, Buchmann N, Gilmanov T, Granier A, Grünwald T, Havránková K, Ilvesniemi H, Janous D, Knohl A, Laurila T, Lohila A, Loustau D, Matteucci G, Meyers T, Miglietta F, Ourcival J-M, Pumpanen J, Rambal S, Rotenberg E, Sanz M, Tenhunen J, Seufert G, Vaccari F, Vesala T, Yakir D, Valentini R. 2005. On the separation of net ecosystem

exchange into assimilation and ecosystem respiration: review and improved algorithm. Glob Change Biol 11:1424–39.

Reichstein M, Bahn M, Ciais P, Frank D, Mahecha MD, Seneviratne SI, Zscheischeler J, Beer C, Buchmann N, Frank DC, Papale D, Ramming A, Smith P, Thonicke K, van der Velde M, Vicca S, Walz A, Wattenbach M. 2013. Climate extremes and the carbon cycle. Nature 500:287–95.

Ricciuto DM, Butler MP, Davis KJ, Cook BD, Bakwin PS, Andrews A, Teclaw RM. 2008. Causes of interannual variability in ecosystem-atmosphere CO_2 exchange in a northern Wisconsin forest using a Bayesian model calibration. Agric For Meteorol 148:309–27.

Richardson AD, Hollinger DY. 2005. Statistical modeling of ecosystem respiration using eddy covariance data: maximum likelihood parameter estimation, and Monte Carlo simulation of model and parameter uncertainty, applied to three simple models. Agric For Meteorol 131:191–208.

Richardson AD, Braswell BH, Hollinger DY, Burman P, Davidson EA, Evans RS, Flanagan LB, Munger JW, Savage K, Urbanski SP, Wofsy SC. 2006. Comparing simple respiration models for eddy flux and dynamic chamber data. Agric For Meteorol 141:219–34.

Richardson AD, Hollinger DY, Aber JD, Ollinger SV, Braswell BH. 2007. Environmental variation is directly responsible for short- but not long-term variation in forest-atmosphere carbon exchange. Glob Change Biol 13:788–803.

Richardson AD, Hollinger DY, Dail DB, Lee JT, Munger W, O'Keefe J. 2009. Influence of spring phenology on seasonal and annual carbon balance in two contrasting New England forest. Tree Physiol 29:321–31.

Schwalm CR, Williams CA, Schaefer K, Anderson R, Arain MA, Baker I, Barr A, Black TA, Chen G, Chen J, Ciais P, Davis KJ, Desai A, Dietze M, Dragoni D, Fischer ML, Flanagan LB, Grant R, Gu L, Hollinger D, Izaurralde RC, Kucharik C, Lafleur P, Law BE, Li L, Li Z, Liu S, Lokupitiya E, Luo Y, Ma S, Margolis H, Matamala R, McCaughey H, Monson RK, Oechel WC, Peng C, Poulter B, Price DT, Riciutto DM, Riley W, Sahoo AK, Sprintsin M, Sun J, Tian H, Tonitto C, Verbeeck H, Verma SB. 2010. A model-data intercomparison of CO_2 exchange across North America: results from the North American Carbon Program site synthesis. J Geophys Res 115:G00H05.

Stoy PC, Katul GG, Siqueira MBS, Juang J-Y, Novick KA, McCarthy HR, Oishi AC, Oren R. 2008. Role of vegetation in determining carbon sequestration along ecological succession in the southeastern United States. Glob Change Biol 14:1–19.

Teklemariam TA, Lafleur PM, Moore TR, Roulet NT, Humphreys ER. 2010. The direct and indirect effects of inter-annual meteorological variability on ecosystem carbon dioxide exchange at a temperate ombrotrophic bog. Agric For Meteorol 150:1402–11.

Tjoelker MG, Oleksyn J, Reich PB. 2001. Modelling respiration of vegetation: evidence for a general temperature-dependent Q_{10}. Glob Change Biol 7:223–30.

Vargas R, Baldocchi DD, Bahn M, Hanson PJ, Hosman KP, Kulmala L, Pumpanen J, Yang B. 2011. On the multi-temporal correlation between photosynthesis and soil CO_2 efflux: reconciling lags and observations. New Phytol 191:1006–17.

Wang Y, Ding G. 2013. Physiological responses of mycorrhizal *Pinus massoniana* seedlings to drought stress and drought resistance evaluation. Chin J Appl Ecol 24:639–45.

Weber U, Jung M, Reichstein M, Beer C, Braakhekke MC, Lehsten V, Ghent D, Kaduk J, Viovy N, Ciais P, Gobron N, Rödenbeck C. 2009. The interannual variability of Africa's ecosystem productivity: a multi-model analysis. Biogeosciences 6:285–95.

Wen X, Wang H, Wang J, Yu G, Sun X. 2010. Ecosystem carbon exchanges of a subtropical evergreen coniferous plantation subjected to seasonal drought, 2003–2007. Biogeosciences 7:357–69.

Wharton S, Chasmer L, Falk M, Paw UKT. 2009. Strong links between teleconnections and ecosystem exchange found at a Pacific Northwest old-growth forest from flux tower and MODIS EVI data. Glob Change Biol 15:2187–205.

Wu J, van der Linden L, Lasslop G, Carvalhais N, Pilegaard K, Beier C, Ibrom A. 2012. Effects of climate variability and functional changes on the interannual variation of the carbon balance in a temperate deciduous forest. Biogeosciences 9:13–28.

Wu C, Chen JM, Black TA, Price DT, Kurz WA, Desai AR, Gonsamo A, Jassal RS, Gough CM, Bohrer G, Dragoni D, Herbst M, Gielen B, Berninger F, Vesala T, Mammarella I, Pilegaard K, Blanken PD. 2013. Interannual variability of net ecosystem productivity in forests is explained by carbon flux phenology in autumn. Glob Ecol Biogeogr 22:994–1006.

Yang B, Pallardy SG, Meyers TP, Gu L-H, Hanson PJ, Wullschleger SD, Heuer M, Hosman KP, Riggs JS, Sluss DW. 2010. Environmental controls on water use efficiency during severe drought in an Ozark Forest in Missouri, USA. Glob Change Biol 16:2252–71.

Yu G, Zhang L, Sun X, Fu Y, Wen X, Wang Q, Li S, Ren C, Song X, Liu Y, Han S, Yan J. 2008. Environmental controls over carbon exchange of three forest ecosystems in eastern China. Glob Change Biol 14:2555–71.

Yuan W, Luo Y, Richardson AD, Oren R, Luyssaert S, Janssens IA, Ceuleman R, Zhou X, Grünwald T, Aubinet M, Berhofer C, Baldocchi DD, Chen J, Dunn AL, Deforest JL, Dragoni D, Goldstein AH, Moors E, Munger JW, Monson RK, Suyker AE, Star G, Scott RL, Tenhunen J, Verma SB, Vesala T, Wofsy SC. 2009. Latitudinal patterns of magnitude and interannual variability in net ecosystem exchange regulated by biological and environmental variables. Glob Change Biol 15:2905–20.

Zhang T, Ren H, Peng S, Yu Z. 1999. The ecological and biological characteristics of *Pinus elliotti*. Ecol Sci 18:8–12.

Zhang J, Wu L, Huang G, Notaro M. 2011a. Relationships between large-scale circulation patterns and carbon dioxide exchange by a deciduous forest. J Geophys Res 116:D04102.

Zhang W, Wang H, Wen X, Yang F, Ma Z, Sun X, Yu G. 2011b. Freezing-induced loss of carbon uptake in a subtropical coniferous plantation in southern China. Ann For Sci 68:1151–61.